Opposite CMIP3/CMIP5 trends in the wintertime Northern Annular Mode explained by combined local sea ice and remote tropical influences

J. Cattiaux[1] and C. Cassou[2]

[1]   A crucial challenge in climate studies is to determine how warming trends due to anthropogenic forcing may affect the natural modes of atmospheric variability. In the northern extratropics, the leading pattern of atmospheric dynamics is known as the Northern Annular Mode (NAM), often computed as the first empirical orthogonal function of sea level pressure (SLP) or geopotential height at 500 mbar (Z500). Here we compare wintertime NAM changes estimated from previous (third phase of the Coupled Model Intercomparison Project (CMIP3)) versus ongoing (fifth phase (CMIP5)) generations of multimodel projections for the 21st century, under similar emission scenarios (A2 scenario versus 8.5 W.m^{-2} Representative Concentration Pathway). CMIP3 projections exhibited a positive NAM trend, albeit this response differed between SLP and Z500, whereas CMIP5 projections rather reveal a negative trend, especially for Z500. We show that the CMIP3/CMIP5 discrepancies are mostly explained in early winter by the local consequence of faster Arctic sea ice loss in CMIP5 and in late winter by the remote influence through teleconnection of stronger warming in the western tropical Pacific. The attribution of CMIP3/CMIP5 discrepancies to the differences in emission scenarios is assessed by investigating NAM responses in common 1% CO_2 idealized experiments.
Citation: Cattiaux, J., and C. Cassou (2013), Opposite CMIP3/CMIP5 trends in the wintertime Northern Annular Mode explained by combined local sea ice and remote tropical influences, *Geophys. Res. Lett.*, *40*, 3682–3687, doi:10.1002/grl.50643.

1.   Introduction

[2]   Annular modes are the leading patterns of extratropical intraseasonal to interannual variability in both Southern and Northern Hemispheres. They are characterized by zonally symmetric meridional seesaws in atmospheric mass between middle and high latitudes [*Thompson and Wallace*, 2000], affecting the strength of the stratospheric polar vortices [*Baldwin et al.*, 1994] and the midlatitude surface westerlies [*Hurrell*, 1995]. In their positive (negative) phase, annular modes correspond to an enhanced (reduced) meridional pressure gradient, therefore strengthening (weakening)

both vortices and westerlies. Assessing how warming trends due to anthropogenic forcing may impact such modes of variability appears to be a crucial issue, particularly in the Northern Hemisphere. Indeed, potential changes in the Northern Annular Mode (NAM)—also referred to as the Arctic Oscillation—would directly influence North American and European land surface climate, especially in boreal winter, through changes in its regional feature known as the North Atlantic Oscillation [*Ambaum et al.*, 2001].

[3]   In the late 1990s, several observational studies reported a trend toward the positive phase of the NAM [e.g., *Thompson et al.*, 2000], consistent with responses found in 21st century projections from general circulation models (GCMs) [e.g., *Fyfe et al.*, 1999], albeit simulated trends were lower than those observed [*Gillett et al.*, 2003]. The complexity of attributing such observed trends to anthropogenic and/or natural forcings given the relatively short periods of record and the presence of strong internal variability was highlighted by *Wunsch* [1999] and further confirmed using GCMs by *Deser et al.* [2012]. In the 2000s, multimodel analyses based on outputs from the third phase of the Coupled Model Intercomparison Project (CMIP3) predicted a positive NAM trend in future projections, associated with decreasing (increasing) sea level pressure (SLP) over polar areas (midlatitudes) [e.g., *Miller et al.*, 2006]. Although the NAM is often considered barotropic, *Woollings* [2008] evidenced that its response to anthropogenic forcing might be baroclinic. Consistently, recent studies dealing with projected Arctic sea ice loss showed that increases in polar ice-free surface heat fluxes would lead to a negative phase of the NAM in altitude while having no clear influence on SLP [e.g., *Deser et al.*, 2010].

[4]   Here we revisit these assertions on the basis of the new generation of GCMs used in the ongoing fifth phase of the Coupled Model Intercomparison Project (CMIP5). Both future changes in SLP and geopotential height at 500 mbar (Z500) are presented to account for potential distinct responses at the surface and aloft. Data and methods are described in section 2. Projected changes in the NAM are investigated in section 3, and section 4 focuses on the origins of CMIP3/CMIP5 differences. Conclusions are discussed in section 5.

2.   Data and Methods

[5]   We use outputs provided by 13 modeling groups having participated to both CMIP3 and CMIP5 exercises (Table S1 in the supporting information). We consider the whole period 1900–2099 by concatenating historical runs over the twentieth century with 21st century projections under A2 scenario (CMIP3, hereafter SA2) and 8.5 W.m^{-2}
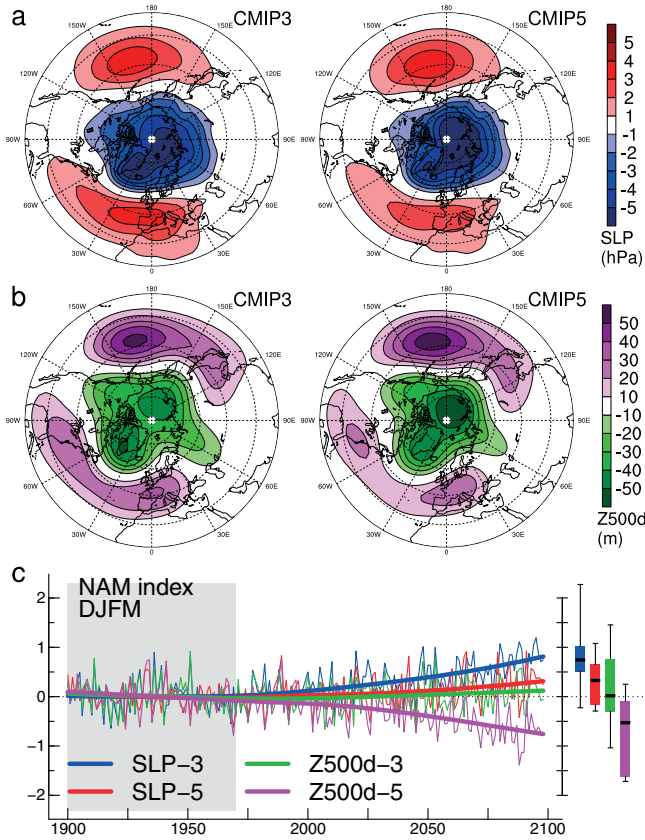

Figure 1. (a) CMIP3 and CMIP5 ensemble mean NAM patterns of SLP, derived from EOF1 of monthly anomalies over DJFM 1950–1999. (b) Same as Figure 1a but for detrended Z500 (Z500d). (c) Ensemble mean NAM indices for DJFM for CMIP3-SA2 (SLP in blue and Z500d in green) and CMIP5-R85 (SLP in red and Z500d in magenta) and associated smoothing splines with 5 degrees of freedom (thick lines). The boxplots (right margin) represent the median (black segment), two-thirds ranges (filled boxes), and full ranges (whiskers) of individual smoothed values in 2099. Individual indices are normalized relative to the period 1900–1970 (gray shading), so that *y* axis units are σ levels.

Representative Concentration Pathway (CMIP5, hereafter R85) scenarios. Idealized 1% CO_2 experiments (hereafter 1PC), available for a subset of nine groups (Table S1), are also analyzed to further isolate the physical mechanisms at work. Only the first member of each experiment (namely *r1i1p1* in the CMIP5 protocol) is considered here. National Centers for Environmental Prediction (NCEP) reanalyses are also used in section 4.2 and Figure S1. Because ensemble mean computations require a common grid, all GCMs atmospheric fields are interpolated onto the regular NCEP 2.5° × 2.5° longitude-latitude grid prior to our analyses.

[6] Following *Miller et al.* [2006], for both SLP and Z500 variables and for each GCM taken separately, we define the winter NAM as the leading empirical orthogonal function (EOF1) constructed from four concatenated monthly (December–March, hereafter DJFM) anomalies over the period 1950–1999 and the Northern Hemisphere poleward of 20°N. Anomalies are computed relative to 1970–1999, and in order to account for the long-term thermal expansion

of the low troposphere, Z500 anomalies are additionally corrected by uniformly removing their spatial averages for each month. NAM indices are derived from the first principal components (PC1), i.e., orthogonal projections of monthly anomalies onto EOF1, and normalized relative to 1900–1970 in order to emphasize long-term trends by the end of the 21st century.

3. Projected Changes in the NAM

[7] On average, CMIP3 models were found to reasonably well represent the SLP NAM pattern derived from NCEP reanalyses [*Miller et al.*, 2006]. Ensemble mean NAM patterns derived from CMIP5 fairly resemble CMIP3 ones for both SLP and Z500 fields (Figures 1a and 1b), thus evidencing the robustness of the NAM representation by the GCMs. A more exhaustive evaluation for individual models is presented in Figure S1. Figure 1c reveals however a clear difference in the DJFM NAM temporal response between CMIP3 and CMIP5 projections. The positive trend for SLP in CMIP3 is much weaker in CMIP5. Differences are even more pronounced for Z500d with virtually no trend found in CMIP3 (ensemble mean and median close to 0
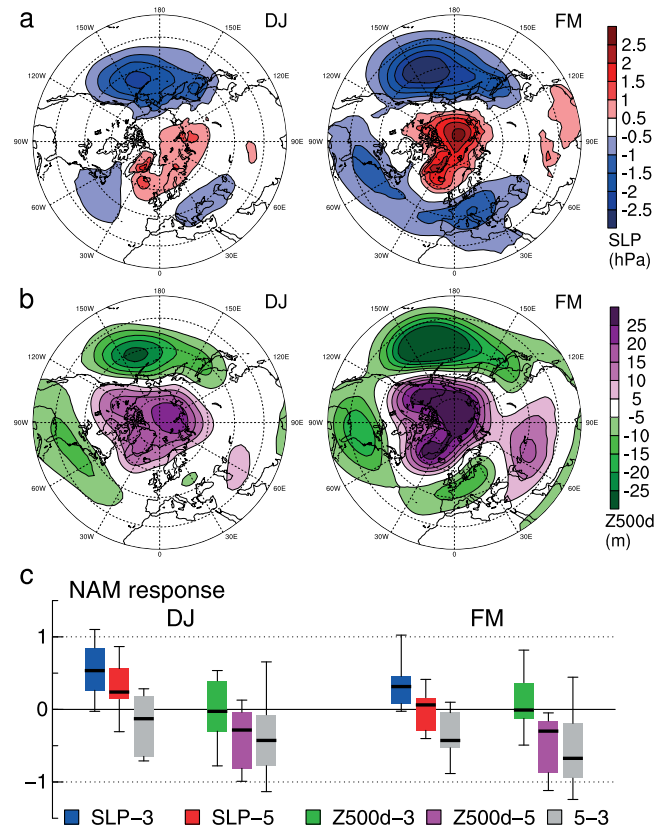

Figure 2. (a) CMIP5–CMIP3 (R85–SA2) difference in ensemble mean SLP projected change (2070–2099 versus 1900-1970) for early (DJ) and late (FM) winter. (b) Same as Figure 2a but for Z500d. (c) Boxplots of individual projected changes in the NAM index for DJ and FM, for CMIP3-SA2 (SLP in blue and Z500d in green) and CMIP5-R85 (SLP in red and Z500d in magenta), with corresponding differences in gray.
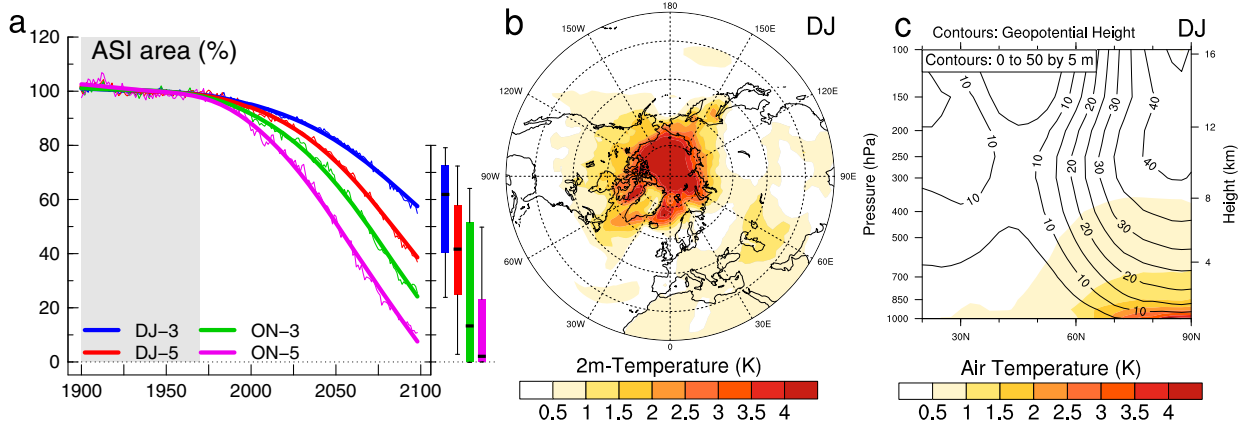
Figure 3. (a) Ensemble mean percentage of Arctic sea ice area for CMIP3-SA2 (DJ in blue and ON in green) and CMIP5-R85 (DJ in red and ON in magenta), with 100% corresponding to the period 1900–1970 (gray shading). Associated smoothing splines with 5 degrees of freedom (thick lines). Boxplots (right margin) as in Figure 1c. (b) CMIP5–CMIP3 (R85–SA2) difference in ensemble mean projected change (2070–2099 versus 1900–1970) in 2 m temperature for DJ. (c) Associated zonal mean projected change in air temperature (colors) and geopotential height (contours).

at the end of the 21st century) in contrast to strong negative trend in CMIP5 projections, with indices falling below -1σ by 2099 for five models out of 13. Although individual NAM responses can highly depend on internal variability, the -0.9σ (-0.5σ) difference between CMIP5 and CMIP3 ensemble mean Z500d (SLP) indices has a probability of 1% (11%) to be obtained by chance, assuming Gaussian distributions for all 13 ensemble members. We verified using five R85 members of our in-house model (CNRM-CM5) that the intermember spread is smaller than the multimodel ensemble spread (not shown), which crudely suggests that intermodel discrepancies dominate the uncertainties. All together, these results are consistent with the weather regime analysis performed by *Cattiaux et al.* [2013] over the North Atlantic sector.

[8] Consistent with CMIP3/CMIP5 discrepancies in the NAM temporal response, the spatial patterns of the CMIP5–CMIP3 difference in winter SLP and Z500d responses—defined as differences between periods 2070–2099 and 1900–1970—project onto the negative phase of the NAM. It is important though to separate the winter season into early (December–January (DJ)) and late (February–March (FM)) months (Figures 2a and 2b). With the exception of the North Pacific area where maximum loading is found throughout winter, SLP anomalies in DJ are weak over the pole while a strong geopotential rise concurrently occurs aloft. Signals are marginal in the North Atlantic sector in DJ, while a broad fully developed hemispheric pattern appears in FM. Accordingly, the CMIP3/CMIP5 discrepancy for winter NAM is stronger in FM than in DJ (Figure 2c) and larger for Z500d than for SLP. CMIP5–CMIP3 NAM differences are negative for all but two models (CSIRO and INGV) in FM for Z500d. Interestingly, no disagreement is found between CMIP3 and CMIP5 in summertime, and the NAM difference gradually builds up from December onward (Figure S2). This suggests a rather baroclinic CMIP3/CMIP5 disagreement in early winter at polar latitudes, followed by a more widespread/hemispheric and barotropic structure in late winter, indicating that underlying processes may differ throughout the season.

4. Origins of the CMIP3/CMIP5 Disagreement

4.1. Early Winter: The Arctic Sea Ice Loss

[9] As reported by J. Stroeve et al. (Trends in Arctic sea ice extent from CMIP5, CMIP3 and observations, submitted to *Geophysical Research Letters*, 2012) for moderate-emission scenarios, a major difference between CMIP3 and CMIP5 projections is the timing of the summer Arctic sea ice loss. Under the CMIP5-R85 scenario, more than half of GCMs included in our ensemble produce nearly ice-free conditions (i.e., remaining area below 5%) in late autumn (October–November (ON)) before the end of the 21st century (four GCMs out of 13 in CMIP3-SA2), and the CMIP3/CMIP5 difference persists throughout early winter (DJ; Figure 3a). For each model, we derive the total sea ice area by multiplying native grid point sea ice fractions by corresponding grid point areas, without any interpolation. Plausible reasons for the faster sea ice loss in our CMIP5 ensemble include (i) new sea ice albedo parameterizations (e.g., melt ponds), (ii) stronger tuning of sea ice simulations to reproduce the recent observed decline (see Stroeve et al. (submitted manuscript, 2012, and references therein) for these two points), and (iii) differences between SA2 and R85 scenarios (discussed in section 4.3). Interestingly, only the two above mentioned GCMs with a positive CMIP5–CMIP3 difference in the NAM response (CSIRO and INGV) make sea ice disappear earlier in CMIP3-SA2 than in CMIP5-R85.

[10] Associated with faster sea ice loss, we find a stronger Arctic amplification in early winter (DJ) in CMIP5-R85 than in CMIP3-SA2, as measured from the 2 m temperature response (Figure 3b). The CMIP5-CMIP3 difference in projected warming is moderate over midlatitudes (0.6 K averaged over the band 30–60°N) while it reaches 3.1 K within the polar circle (66–90°N), locally exceeding 5 K over marine areas. This warm surface anomaly expands upward into the midtroposphere over the pole, CMIP5 warming being 1 K (0.5 K) higher than CMIP3 at 700 mbar (500 mbar; Figure 3c). The enhanced Arctic amplification in CMIP5 results in a greater rise of the midtroposphere geopotential over the pole (30 m at 500 mbar) than over
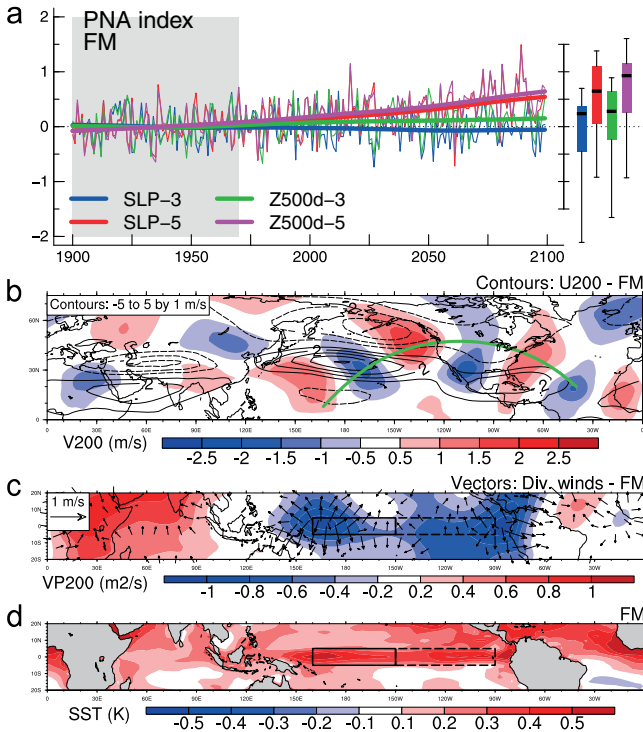
Figure 4. (a) Same as Figure 1c but for PNA indices in FM. (b) CMIP5–CMIP3 (R85–SA2) difference in ensemble mean projected change in zonal (contours) and meridional (colors) winds at 200 mbar for FM. (c) Same for the velocity potential (colors) and divergent wind components at 200 mbar. (d) Same for the sea surface temperature. The green great circle in Figure 4b symbolizes the Rossby wave. The boxes in Figures 4c and 4d depict the Niño-3 (dashed) and Niño-4 (solid) regions.

midlatitudes (7 m), whereas the geopotential response is weakly impacted at the surface in agreement with both SLP and Z500d patterns found for DJ in Figure 2. Both vertical structure and timing (i.e., response delayed to early winter) of differences in temperature and geopotential responses are consistent with the results of sensitivity experiments conducted in *Deser et al.* [2010], where climatological and nearly ice-free Arctic conditions are contrasted (see their Figure 13). This indicates that the CMIP3/CMIP5 disagreement in the NAM response in early winter likely results in part from the more rapid Arctic sea ice loss in CMIP5.

4.2. Late Winter: The North Pacific Teleconnection

[11] In FM, the influence of autumn Arctic sea ice, albeit present, diminishes (Figure S2), and the hemispheric and barotropic structure of the CMIP3/CMIP5 discrepancy (Figure 2) suggests that underlying causes may involve more global dynamical features. The strongest discrepancy found in the North Pacific in both SLP and Z500d responses is now fully developed and strongly projected onto the positive phase of the leading pattern of the regional variability, characterized by anomalously high (low) pressures over the subtropical Pacific and Western Canada (North Pacific and Florida), and known as the Pacific-North American (PNA) pattern [*Wallace and Gutzler*, 1981]. Figure 4a shows that all CMIP5-R85 members present a barotropic positive tendency for the PNA, with the exception of MIROC, while

CMIP3-SA2 projections did not exhibit any systematic trend. For both SLP and Z500d, PNA indices are computed similarly to NAM indices (Figure 1), except that the pattern is derived from the second rotated EOF (REOF2) instead of the EOF1 and that we use NCEP reanalyses to derive reference patterns since PNA patterns are not systematically found for the same REOF across GCMs.

[12] At interannual and larger timescales, the observed late winter PNA variability has been shown to be strongly forced by the tropical Pacific [*Horel and Wallace*, 1981]. *Cassou and Terray* [2001], among others, provide evidence from models that positive PNA would tend to favor negative NAM associated with an equatorward shift of the midlatitude jet stream over the North Pacific and North Atlantic sectors. Here such a southward shift of the jet is found in the CMIP3/CMIP5 difference of the 200 mbar zonal wind response; it is in link to a Rossby wave train emerging from the western Pacific and propagating along a great circle as revealed by alternating opposite sign 200 mbar meridional wind cores (Figure 4b) [*Branstator*, 2002]. This wave structure originates from enhanced upper level divergence in CMIP5 in the central tropical Pacific (Niño-4 region), known to be a key region to trigger midlatitude teleconnections (Figure 4c) [*Barsugli and Sardeshmukh*, 2002], and is associated with stronger surface oceanic warming of the whole tropical Pacific in CMIP5 than in CMIP3 (Figure 4d). Additional upper level divergence also occurs in the eastern basin (Niño-3 region), and the associated Rossby wave tends to extend/reinforce the central Pacific generated one deeper into the Atlantic. Our results thus indicate that the CMIP3/CMIP5 disagreement in the NAM response in late winter likely results from the stronger tropical Pacific warming in CMIP5 that remotely impacts the extratropical dynamics through the PNA teleconnection. The latter is moderately present in DJ, but it is overly dominant and fully developed in FM (Figure S2) and could even contribute to the greater late winter Arctic sea ice loss in CMIP5 (J. J. Wettstein and C. Deser, Internal variability in projections of twenty-first century Arctic sea ice loss: Role of the large-scale atmospheric circulation, submitted to *Journal of Climate*, 2013).

4.3. Changes in Emission Scenario Versus Model Characteristics

[13] Potential reasons for both faster autumn Arctic sea ice melt and greater late winter tropical Pacific warming in CMIP5 include the fact that CMIP3-SA2 and CMIP5-R85 scenarios are not strictly identical; the latter cause is tested using available 1PC experiments shared by both exercises (Table S1). In 1PC, the CMIP3/CMIP5 disagreement in the winter NAM response only concerns the Z500d index, while CMIP3 and CMIP5 SLP indices share a similar positive trend (Figure 5a). As for SA2/R85 scenarios, the CMIP3/CMIP5 difference in the 1PC Z500d response is characterized by lower geopotential in the North Pacific sector and significant greater rise over the pole in early winter associated with a stronger Arctic amplification caused by a faster autumn sea ice melt in CMIP5-1PC (Figures 5b and 5c). But conversely to SA2/R85 scenarios, we find no tendency in the late winter PNA pattern in 1PC experiments (not shown). Accordingly, the response in 200 mbar winds does not significantly differ between CMIP3 and CMIP5 over the North Pacific (Figure 5d). Interestingly,
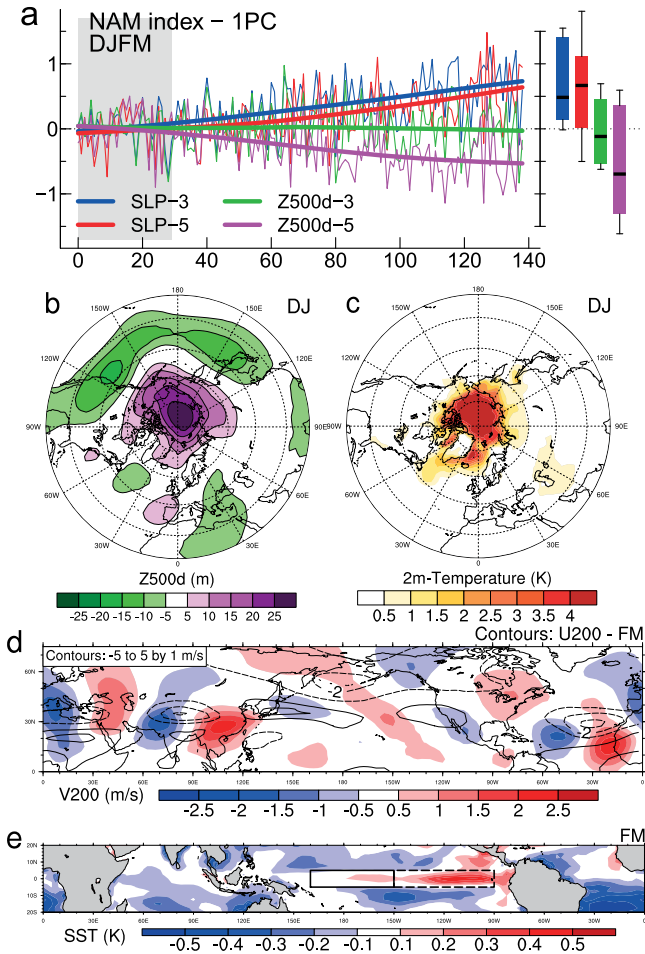
Figure 5. Same as (a) Figure 1c, (b) Figure 2b, (c) Figure 3b, (d) Figure 4b, and (e) Figure 4d but for 1PC experiments (i.e., 140 year simulations with increments of 1% CO_2 per year). The NAM indices in Figure 5a are normalized relative to the first 30 years (gray shading). Responses in other panels are differences between the last and the first 30 years.

only the Niño-3 part of the stronger oceanic warming found in Figure 4d remains in Figure 5e for 1PC, thus confirming that the Rossby wave train found in Figure 4b clearly originates from the Niño-4 area while Niño-3 plays a minor role. We verified that differences between SA2/R85 and 1PC results do not arise from the four missing GCMs in 1PC ensembles (Figure S3).

5. Discussion and Conclusions

[14]   In this paper, we have investigated the CMIP3-SA2 and CMIP5-R85 projected changes in the NAM by the end of the 21st century in terms of SLP and Z500. We show that the positive trend found at the surface in CMIP3 contrasts with the absence of trend found in CMIP5. Those changes are strongly amplified along the vertical. We associate this CMIP3/CMIP5 disagreement with (i) the delayed Arctic sea ice freezing in early winter in CMIP5, leading to locally stronger thermal expansion of the lower troposphere and a rather baroclinic signal, and (ii) the higher warming in the western/central tropical Pacific in late winter in CMIP5, leading to positive PNA through teleconnection processes

and *in fine* negative NAM. Additional results from 1PC experiments reveal that while discrepancies in the western tropical Pacific warming are likely to arise from the difference between SA2 and R85 scenarios, the higher sensitivity of Arctic sea ice to CO_2 forcing in CMIP5 GCMs rather results from model properties of the new generation. Our results suggest that even if the temptation is high to compare (or worse combine) SA2 and R85 scenarios outputs, one has to be extremely cautious in the deduced conclusions.

[15]   Other possible causes of the CMIP3/CMIP5 discrepancy in the NAM response remain to be investigated, including the respective roles of stratospheric ozone representation [e.g., *Morgenstern et al.*, 2010] and increased horizontal and vertical atmospheric resolutions in GCMs [e.g., *Roeckner et al.*, 2006]. In particular, strong connections between the tropospheric NAM and the stratospheric polar vortex [*Thompson and Wallace*, 2000] highlight the importance of a well-resolved stratosphere in the NAM simulation, albeit E. Manzini et al. (Role of the stratosphere in Northern winter climate change as simulated by the CMIP5 models, submitted to *Journal of Geophysical Research*, 2006) found no clear distinction between NAM responses of high- and low-top models in CMIP5.

[16]   Finally, one crucial issue consists in assessing whether changes evidenced in future projections already occur in recent observations. The positive NAM trend detected by *Gillett et al.* [2003] in SLP over 1948–1998 has considerably weakened over recent years, marked by episodes of exceptionally negative NAM [*Cattiaux et al.*, 2010; *L'Heureux et al.*, 2010]. So far, only Arctic sea ice decline is clearly detectable, but although concurrent with the weakening of the NAM trend, its influence on atmospheric dynamics remains under discussion [*Francis et al.*, 2009; *Screen et al.*, 2012]. However, since autumn ice-free conditions could actually arrive earlier than in model projections (Stroeve et al., submitted manuscript, 2012), the baroclinicity in the NAM response might become discernible in the next few decades.

References

Ambaum, M., B. Hoskins, and D. Stephenson (2001), Arctic Oscillation or North Atlantic Oscillation? *J. Clim.*, *14*, 3495–3507.

Baldwin, M., X. Cheng, and T. Dunkerton (1994), Observed correlations between winter-mean tropospheric and stratospheric circulation anomalies, *Geophys. Res. Lett.*, *21*(12), 1141–1144.

Barsugli, J., and P. Sardeshmukh (2002), Global atmospheric sensitivity to tropical SST anomalies throughout the Indo-Pacific basin, *J. Clim.*, *15*(23), 3427–3442.

Branstator, G. (2002), Circumglobal teleconnections, the jet stream waveguide, and the North Atlantic Oscillation, *J. Clim.*, *15*(14), 1893–1910.

Cassou, C., and L. Terray (2001), Oceanic forcing of the wintertime low-frequency atmospheric variability in the North Atlantic European sector: A study with the ARPEGE model, *J. Clim.*, *14*, 4266–4291.

Cattiaux, J., R. Vautard, C. Cassou, P. Yiou, V. Masson-Delmotte, and F. Codron (2010), Winter 2010 in Europe: A cold extreme in a warming climate, *Geophys Res. Lett.*, *37* (20), doi:10.1029/2010GL044613a.

Cattiaux, J., H. Douville, and Y. Peings (2013), European temperatures in CMIP5: Origins of present-day biases and future uncertainties, *Clim. Dyn.*, published online, doi:10.1007/s00382- 013-1731-y.

Deser, C., R. Tomas, M. Alexander, and D. Lawrence (2010), The seasonal atmospheric response to projected Arctic sea ice loss in the late twenty-first century, *J. Clim.*, *23*, 333–351, doi:10.1175/2009JCLI3053.1.

Deser, C., A. Phillips, V. Bourdette, and H. Teng (2012), Uncertainty in climate change projections: The role of internal variability, *Clim. Dyn.*, *38*, 527–546, doi:10.1007/s00382-010-0977-x.

Francis, J., W. Chan, D. Leathers, J. Miller, and D. Veron (2009), Winter Northern Hemisphere weather patterns remember summer Arctic sea-ice extent, *Geophys. Res. Lett.*, *36*, L07503, doi:10.1029/2009GL037274.

Fyfe, J., G. Boer, and G. Flato (1999), The Arctic and Antarctic oscillations and their projected changes under global warming, *Geophys. Res. Lett.*, *26*(11), 1601–1604.

Gillett, N., F. Zwiers, A. Weaver, and P. Stott (2003), Detection of human influence on sea-level pressure, *Nature*, *422*(6929), 292–294, doi:10.1038/nature01487.

Horel, J., and J. Wallace (1981), Planetary-scale atmospheric phenomena associated with the interannual variability of sea surface temperature in the equatorial Pacific, *Mon. Weather Rev.*, *109*, 813–829.

Hurrell, J. (1995), Decadal trends in the North Atlantic Oscillation: Regional temperatures and precipitation, *Science*, *26*, 676–679.

L'Heureux, M., A. Butler, B. Jha, A. Kumar, and W. Wang (2010), Unusual extremes in the negative phase of the Arctic Oscillation during 2009, *Geophys. Res. Lett.*, *37*, L10704, doi:10.1029/2010GL043338.

Miller, R., G. Schmidt, and D. Shindell (2006), Forced annular variations in the 20th century Intergovernmental Panel on Climate Change Fourth Assessment Report models, *J. Geophys. Res.*, *111*, D18101, doi:10.1029/2005JD006323.

Morgenstern, O., et al. (2010), Anthropogenic forcing of the Northern Annular Mode in CCMVal-2 models, *J. Geophys. Res.*, *115*(D00M03), doi:10.1029/2009JD013347.

Roeckner, E., R. Brokopf, M. Esch, M. Giorgetta, S. Hagemann, L. Kornblueh, E. Manzinim, U. Schlese, and U. Schulzweida (2006), Sensitivity of simulated climate to horizontal and vertical resolution in the ECHAM5 atmosphere model, *J. Clim.*, *19*, 3771–3791, doi:10.1175/JCLI3824.1.

Screen, J., I. Simmonds, C. Deser, and R. Tomas (2012), The atmospheric response to three decades of observed Arctic sea ice loss, *J. Clim.*, *26*, 1230–1248, doi:10.1175/JCLI-D-12-00063.1.

Thompson, D., and J. Wallace (2000), Annular modes in the extra-tropical circulation. Part I: Month-to-month variability, *J. Clim.*, *13*(5), 1000–1016, doi:10.1175/1520-0442(2000)013.

Thompson, D., J. Wallace, and G. Hegerl (2000), Annular modes in the extratropical circulation. Part II: Trends, *J. Clim.*, *13*, 1018–1036.

Wallace, J., and D. Gutzler (1981), Teleconnections in the geopotential height field during the Northern Hemisphere winter, *Mon. Weather Rev.*, *109*(4), 784–812.

Woollings, T. (2008), Vertical structure of anthropogenic zonal-mean atmospheric circulation change, *Geophys. Res. Lett.*, *35*, L19702, doi:10.1029/2008GL034883.

Wunsch, C. (1999), The interpretation of short climate records, with comments on the North Atlantic and Southern Oscillations, *Bull. Am. Meteor. Soc.*, *80*, 245–256.